Physics – Uspekhi **42** (6) 563 – 572 (1999)

PHYSICS OF OUR DAYS PACS numbers: **95.30.-k, 98.80.-k**, 98.80.Ft

The puzzle of the lightest elements: observations, predictions, hypotheses

Ya M Kramarovskiĭ, V P Chechev

Contents

Abstract. The prediction that deuterium and helium-3 are produced in cosmological nuclear fusion, together with recent data on their interstellar abundance, have attracted the attention of astrophysicists to models of how these nuclides were produced and destroyed back at the Galaxy's pre-stellar stage. In particular, the question of whether the observed yields of D and ^{3}He can be employed to pose restrictions on the Standard Model of Big Bang nucleosynthesis is being actively discussed. In this work some aspects of this problem are discussed.

1. Big Bang nucleosynthesis

1.1. The standard model predictions

A key parameter of the so-called 'standard model' that describes the behavior of matter and its composition during the primordial nucleosynthesis is the dimensionless ratio of the baryon matter density (n_b) to the photon number density which are in equilibrium with matter at that epoch. This parameter is usually denoted by the greek letter $\eta = n_b/n_\gamma$ or (in the units 10^{-10}) $\eta_{10} = 10^{10}\eta$.

According to the standard model, the primordial (cosmological) nucleosynthesis begins when the hot Universe cools to a temperature of ~ 0.8 MeV. At higher temperatures ($T \gg 0.8$ MeV), equilibrium weak interaction reactions converting neutrons into protons and vice versa take place in the Universe:

$$\mathrm{n} + \nu \rightarrow \mathrm{p} + \mathrm{e}^-, \quad \mathrm{n} + \mathrm{e}^+ \rightarrow \mathrm{p} + \bar{\nu}, \quad \mathrm{n} \rightarrow \mathrm{p} + \mathrm{e}^- + \bar{\nu}. \quad (1)$$

Weak interactions at $T \gg 0.8$ MeV are sufficiently fast to support the statistical equilibrium $n/p = \exp(-Q/T)$, where n/p is the ratio of neutron to proton number densities and Q is the difference between the neutron and proton masses ($Q = 1.293$ MeV). At some moment during the Universe expansion and cooling (~ 1 s) these weak interaction reactions becomes insufficiently rapid to maintain the equilibrium.

The equilibrium freezes out and the neutron-to-proton ratio deviates from the equilibrium value. Due to neutron decay the ratio n/p slightly decreases during the subsequent expansion as shown in Fig. 1 [1].

At a temperature of ~ 0.07 MeV all neutrons are bound into synthesized nuclei and the number of neutrons becomes constant.

The duration of weak interaction reactions in the equilibrium hot Universe is a function of temperature, $\tau = nT^{-5}$, and the Universe expansion rate is $t = aT^{-2}$, where t is the time since the beginning of expansion [2]. Therefore, the freezing-out of the equilibrium occurs at a temperature $t = \tau$, with $T_f = (b/a)^{1/3}$ and a and b being

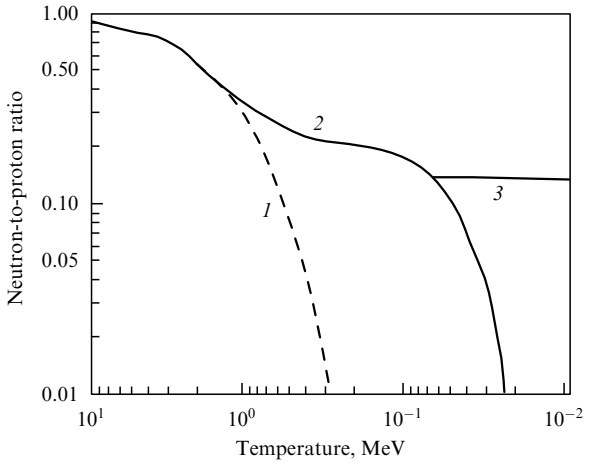

Figure 1. Change of the neutron-to-proton ratio with temperature. Nuclear statistical equilibrium (NSE) is shown by the dashed curve *1*. If only neutron decay occurs (all other reactions are 'frozen'), the n/p ratio follows the curve 2. The true final n/p ratio is shown by curve *3* [1].

Ya M Kramarovskiĭ, V P Chechev V G Khlopin Radium Institute, 2nd Murinskiĭ prosp. 28, 194021 St. Petersburg
Tel. (812) 247-37-06. Fax (812) 247-80-95

Received 20 August 1998, revised 1 March 1999
Uspekhi Fizicheskikh Nauk **169** (6) 643 – 652 (1999)
Translated by K A Postnov; edited by S D Danilov

independent of temperature (T_f is around ~ 1 MeV in the standard model). Note that the parameter b related to the weak interaction rate (as well as to the neutron life time τ_n) determines the temperature of 'decoupling' of weak interaction reactions and thus the n/p ratio by the beginning of nucleosynthesis. Ultimately, this parameter determines the abundance of the produced ^{4}He, the main product of the primordial nucleosynthesis. The list of nuclear reactions leading to ^{4}He formation includes the consecutive transformations $p(n,\gamma)D$, $D(n,\gamma)^3H$, $D(p,\gamma)^3He$, $^3He(n,\gamma)^4He$, $^3H(p,\gamma)^4He$.

In Figure 2 we plot the light element yields including deuterium (D), tritium (^{3}H), and helium (^{3}He, ^{4}He) as a function of temperature in the hot Universe. The curves were calculated in Ref. [1] for the chosen parameter $\eta = 10^{-9.5}$ ($\eta_{10} = 3.16$). Here we wish to reproduce the interpretation of these curves given in Ref. [1]. There are four kinds of deviations from the nuclear statistical equilibrium (NSE): at $T = 0.8$, 0.6, 0.2, and 0.07 MeV. At temperatures higher than 0.6 MeV ^{4}He is in NSE-equilibrium with ^{3}He and ^{3}H, and ^{3}He is in equilibrium with ^{3}H, both nuclei being in equilibrium with D. At the same time, the nuclei of deuterium are in equilibrium with neutrons and protons. The mass ratios of the four nuclei are

$$X_D = 16.3\left(\frac{T}{m_n}\right)^{3/2}\exp\left(\frac{2.22}{T}\right)X_n X_p\,,$$

$$X_{^3H} = 57.4\left(\frac{T}{m_n}\right)^{3/2}\exp\left(\frac{8.50}{T}\right)X_n^2 X_p\,,$$

$$X_{^3He} = 16.3\left(\frac{T}{m_n}\right)^{3/2}\exp\left(\frac{7.72}{T}\right)X_n X_p^2\,,$$

$$X_{^4He} = 113\left(\frac{T}{m_n}\right)^{9/2}\exp\left(\frac{28.3}{T}\right)X_n^2 X_p\,. \qquad (2)$$

In these relations X_j denote the mass fractions of the corresponding nuclei and nucleons, T is the temperature in MeV, and m_n is the nucleon mass in MeV. The numbers in the exponents stand for the nucleon binding energies in MeV. The NSE-yields are shown in Fig. 2 by dashed curves.

As seen from Fig. 2, ^{4}He follows its NSE-yield curve down to $T \sim 0.6$ MeV, and if statistical equilibrium were conserved, its yield would strongly dominate over all other nuclei. This does not occur, however, since its production is limited by the creation rates of ^{3}H and ^{3}H. At $T \sim 0.6$ MeV reactions

$$^3He(n,\gamma)\,^4He \quad \text{and} \quad ^3H(p,\gamma)\,^4He \qquad (3)$$

become too slow to maintain NSE-equilibrium and the ^{4}He yield deviates from the NSE-track. By that time the reverse reaction rates in (3) drop sharply with respect to the direct reaction ones (see Fig. 3). Then ^{4}He follows along the NSE-curves for nuclei with the mass 3 (^{3}He, ^{3}H) until it meets new constraints at $T \sim 0.2$ MeV which are connected with the 'freezing-out' of equilibrium of ^{3}H, ^{3}He with deuterium and are maintained due to the reactions

$$D(n,\gamma)\,^3He; \quad D(p,\gamma)\,^3He\,. \qquad (4)$$

In a similar way, the yields of ^{3}H, ^{3}He are constrained by the D formation rate and their curves (and ^{4}He) follow along the deuterium NSE-curve.

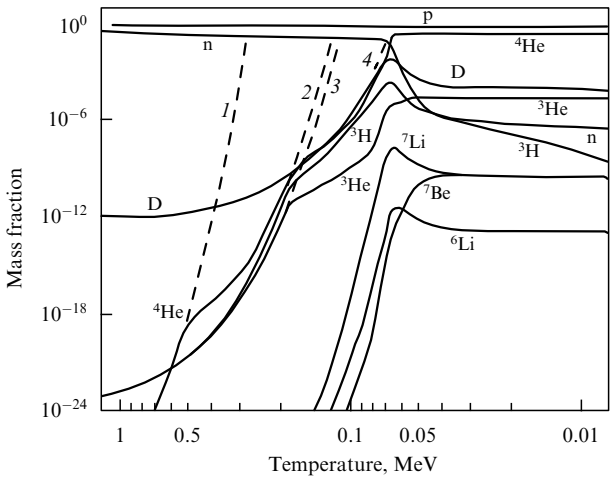

Figure 2. Change of the light element yields with temperature for baryon-to-photon ratio $\eta_{10} = 3.16$. The dashed curves (*1–4*) indicate ^{4}He, ^{3}H, ^{3}He, and D yields in nuclear statistical equilibrium, respectively.

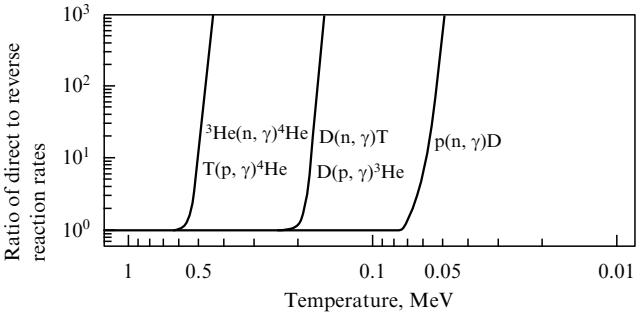

Figure 3. Ratio of direct to reverse reaction rates in the light element nucleosynthesis [1].

The fourth deviation from nuclear statistical equilibrium occurs near 0.07 MeV where the rate of reaction $p(n,\gamma)D$ decreases with further expansion (Fig. 3). One can also note one more deviation at $T \sim 0.08$ MeV where tritium and helium-4 stop interacting with each other through reaction ^{3}He(n, p)^{3}H.

Smith, Kawano and Malany [1] provide a detailed numerical analysis of the modern state of experimental data on the primordial nucleosynthesis thermonuclear reaction rates for typical temperatures in the standard hot Universe model. They were the first to consider the accuracies of these reaction rates and used recent results of neutron life time measurements. Figures 4–7 depict the most important creation and destruction rates of D, ^{3}H, ^{3}He and ^{4}He calculated in Ref. [1]. It is seen that evolution of the lightest element yields occurs in the temperature range from 0.01 to 1 MeV. The main differences from previous analyses (see, e.g., Ref. [3]), which are due to new laboratory measurements of the reaction cross-sections, are concerned with ^{3}He and ^{4}He production. Reaction D(D,γ)^{4}He, which was considered earlier to be important for ^{4}He production, is practically negligible. ^{4}He is mainly created via the thermonuclear reaction T(D, n)^{4}He and the reaction ^{3}He(n,γ)^{4}He. In turn, ^{3}H is formed almost in equal amounts by the reaction ^{3}He(n, p)^{3}H, as well as by reaction D(D, p)^{3}H which was previously thought to be the principal one.

Figure 8 presents the main reactions with nucleons that lead to the nucleosynthesis of the discussed nuclei up to ^{4}He [4]. The use of the laboratory cross-sections to calculate these

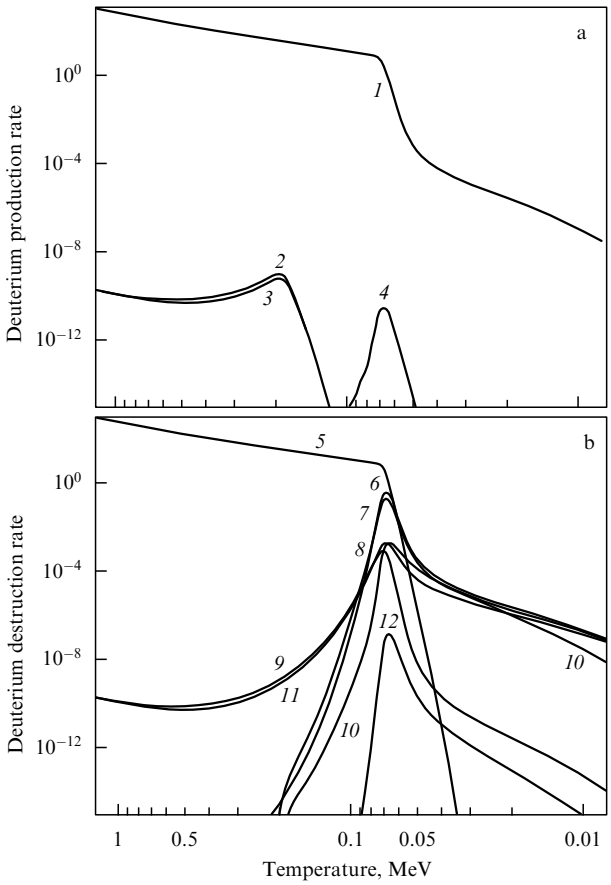

Figure 4. Rate of most important reactions leading to the production (a) and destruction (b) of deuterium [1]: *1* — p(n, γ)D, *2* — ^{3}He(γ, p)D, *3* — T(γ, n)D, *4* — ^{6}Li(γ, α)D, *5* — D(γ, n)p, *6* — D(T, n)^{4}He, *7* — D(D, n)^{3}He, *8* — D(D, p)T, *9* — D(p, γ)^{3}He, *10* — D(^{3}He, p)^{4}He, *11* — D(n, γ)T, *12* — D(^{7}Li, nα)^{4}He.

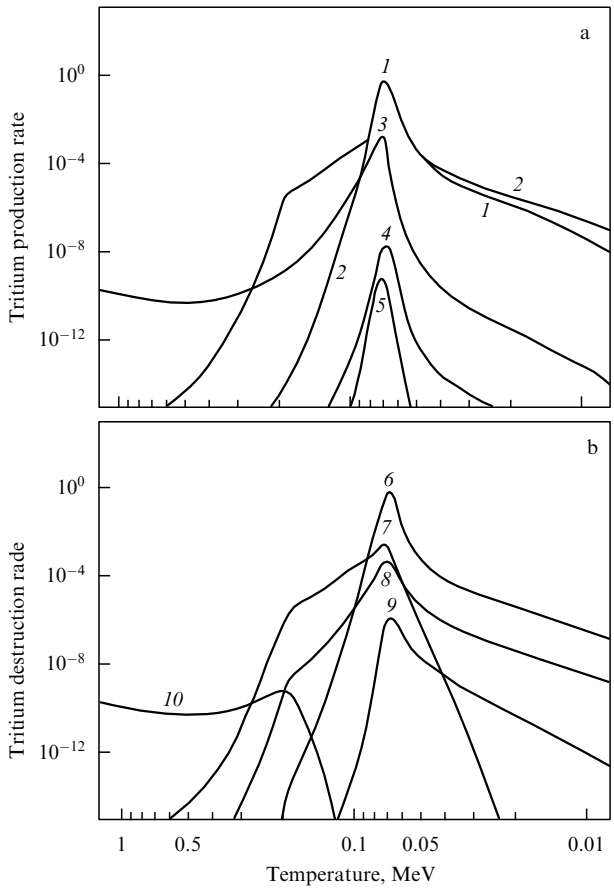

Figure 5. Rate of most important reactions leading to the production (a) and destruction (b) of tritium [1]: *1* — ^{3}He(n, p)T, *2* — D(D, p)T, *3* — D(n, γ)T, *4* — ^{6}Li(n, α)T, *5* — ^{7}Li(γ, α)T, *6* — T(D, n)^{4}He, *7* — T(p, n)^{3}He, *8* — T(pγ)^{4}He, *9* — T(α, γ)^{7}Li, *10* — T(γ, n)D.

reaction rates in the primordial nucleosynthesis is somewhat different from the procedure applied when studying stellar nucleosynthesis due to the need of averaging down to much lower energies

$$N_A\langle\sigma v\rangle \propto T^{-3/2}\int_0^\infty \sigma(E)E\exp\left(-\frac{E}{kT}\right)\mathrm{d}E, \qquad (5)$$

where T is the plasma temperature, E is the particle energy, N_A is the Avogadro number, $N_A\langle\sigma v\rangle$ is the density-independent reaction rate. For charged particles with cross-sections depending exponentially on the energy due to passing the Coulomb barrier, the result of integration of the above equation has a peak at an effective energy E_0 with a width ΔE_0, where

$$E_0 = 122A^{1/3}(Z_1Z_2)^{2/3}T_9^{2/3}\ \mathrm{keV},$$
$$\Delta E_0 = 237A^{1/6}(Z_1Z_2)^{1/3}T_9^{5/6}\ \mathrm{keV}.$$

The reaction D(D, n) ^{3}He provides an example showing how low energies should be taken into account in the primordial nucleosynthesis: $E_0 = 6$ keV, $\Delta E_0 = 0.5$ keV at $T_9 = 0.01$ MeV; $E_0 = 122$ keV, $\Delta E_0 = 0-360$ keV at $T_9 = 1.0$ MeV, and $E_0 = 360$ keV, $\Delta E_0 = 0-1260$ keV at $T_9 = 5.0$ MeV. Fig. 9 demonstrates mass fractions of ^{4}He, D/H, (D + ^{3}HE)/H, ^{7}Li/H calculated as a function of the baryon-to-photon ratio [1]. The dashed curves show 2-σ errors in the calculated yields. These calculations are performed using Monte-Carlo analysis with account of corrections due to numerical errors.

1.2 Comparison of the observed and predicted yields of deuterium and helium

A comparison of light element yields predicted by the standard model with primordial yields that can be evaluated from modern observations enable us to put constraints on the basic parameter of the Big Bang nucleosynthesis (BBN) theory. To this end, we consider estimates of the primordial yields of D, ^{3}He and ^{4}He using the analysis as in Ref. [1] but with account of more recent observational data on D and ^{3}He.

1.2.1 Observations

a) Primordial deuterium. Deuterium is the most fragile of the light elements due to its small charge and low stability ($E_{coup} = 2.22$ MeV). It is destroyed in stellar interiors at temperatures 0.5×10^6 K while the critical temperatures for other nuclei are much higher:

$$T_{cr}(^3\mathrm{He}) \sim 7\times10^6\ \mathrm{K},\quad T_{cr}(^6\mathrm{Li}) \sim 2.0\times10^6\ \mathrm{K},$$
$$T_{cr}(^7\mathrm{Li}) \sim 2.5\times10^6\ \mathrm{K},\quad T_{cr}(^9\mathrm{Be}) \sim 3.5\times10^6\ \mathrm{K},$$
$$T_{cr}(^{11}\mathrm{Be}) \sim 5.0\times10^6\ \mathrm{K},\quad T_{cr}(^{10}\mathrm{Be}) \sim 5.3\times10^6\ \mathrm{K}. \qquad (6)$$

So it is usually thought that all the primordial deuterium which was present in the primary interstellar medium was

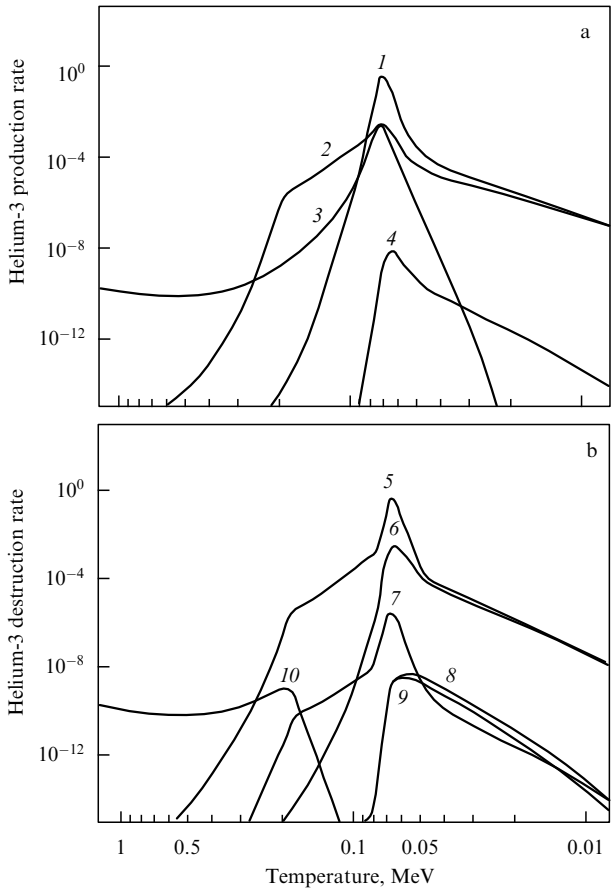

Figure 6. Rate of most important reactions leading to the production (a) and destruction (b) of helium-3 [1]: *1* — $D(D,n)^3He$, *2* — $T(p,n)^3He$, *3* — $D(p,\gamma)^3He$, *4* — $^6Li(p,\alpha)^3He$, *5* — $^3He(n,p)T$, *6* — $^3He(D,p)^4He$, *7* — $^3He(n,\gamma)^4He$, *8* — $^3He(^3He,2p)^4He$, *9* — $^3He(D,\gamma)^7Be$, *10* — $^3He(\gamma,p)D$.

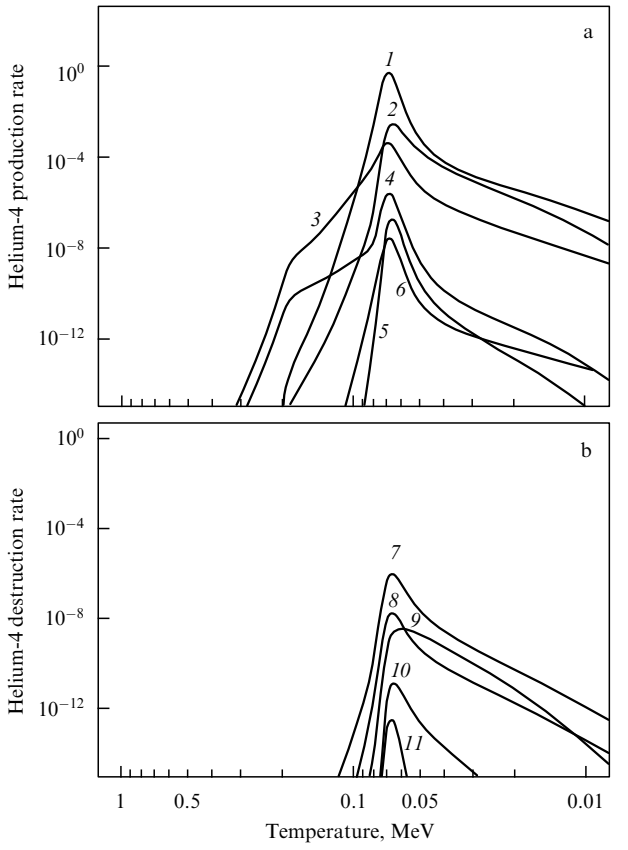

Figure 7. Rate of most important reactions leading to the production (a) and destruction (b) of helium-4 [1]: *1* — $^4He(T,\gamma)^7Li$, *2* — $^4He(D,\gamma)^6Li$, *3* — $^4He(^3He,\gamma)^7Be$, *4* — $^4He(^7Li,\gamma)^{11}B$, *5* — $^4He(^6Li,n)^{11}B$, *6* — $T(D,n)^4He$, *7* — $^3He(D,p)^4He$, *8* — $T(p,\gamma)^4He$, *9* — $^3He(n,\gamma)^4He$, *10* — $^7Li(D,n\alpha)^4He$, *11* — $D(D,\gamma)^4He$.

destroyed and converted into ^3He. Although some models for deuterium production in galactic objects have been proposed (see, for example, Refs [5, 6]), none of them has been widely accepted. (The main arguments against the stellar production of deuterium are given in Ref. [7]).

If deuterium only starts being destroyed immediately after the primordial nucleosynthesis epoch, its modern abundance can be taken as a strict lower limit to the primordial yields D_{BB} (here and below index BB indicates the BBN epoch). Since the predicted standard primordial deuterium yield rapidly decreases with the baryon-to-photon ratio (see Fig. 9), the value of D_{BB} is used as an upper bound on η.

Observations of deuterium inside the Solar system (in meteorites and solar wind) give its modern abundance as $(2.6 \pm 1.0) \times 10^{-5}$ [8]. In extrasolar objects D was first observed in the form of the molecules CH_3D in the Jovian atmosphere [9]. It was also discovered in the form of the molecule DCN in galactic molecular clouds [10] and in the form of HD and DI in diffuse clouds [11, 12]. Extensive data was later collected by the Copernicus satellite which observed deuterium Lyman absorption lines from distances of up to 1 kpc. According to these observations, $D/H = 5 \times 10^{-6} - 2 \times 10^{-5}$. The most recent measurements of the present-day deuterium abundance in the local interstellar medium (ISM) obtained by the Hubble Space Telescope yield $D/H = (1.65 \pm 0.07) \times 10^{-5}$ [12] and $D/H \sim 10^{-5}$ in another direction [13].

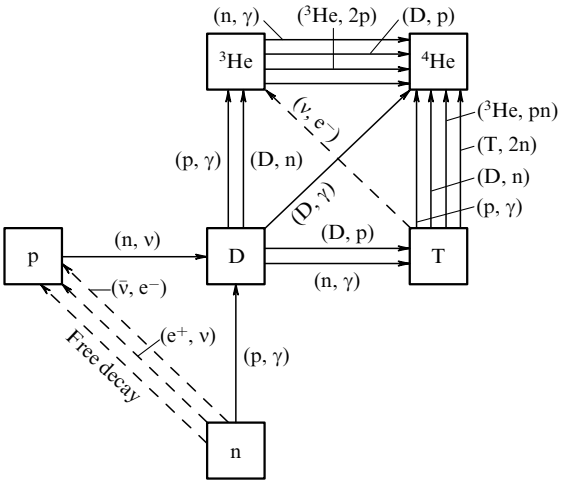

Figure 8. Primordial nucleosynthesis reactions producing the lightest elements [4].

Thus we can accept the present-day deuterium abundance to be

$$D/H > (1.6 \pm 0.1) \times 10^{-5},$$

which is a lower limit to D_{BB}.

In 1994 deuterium was observed for the first time in very remote objects in the Universe. These observations were made

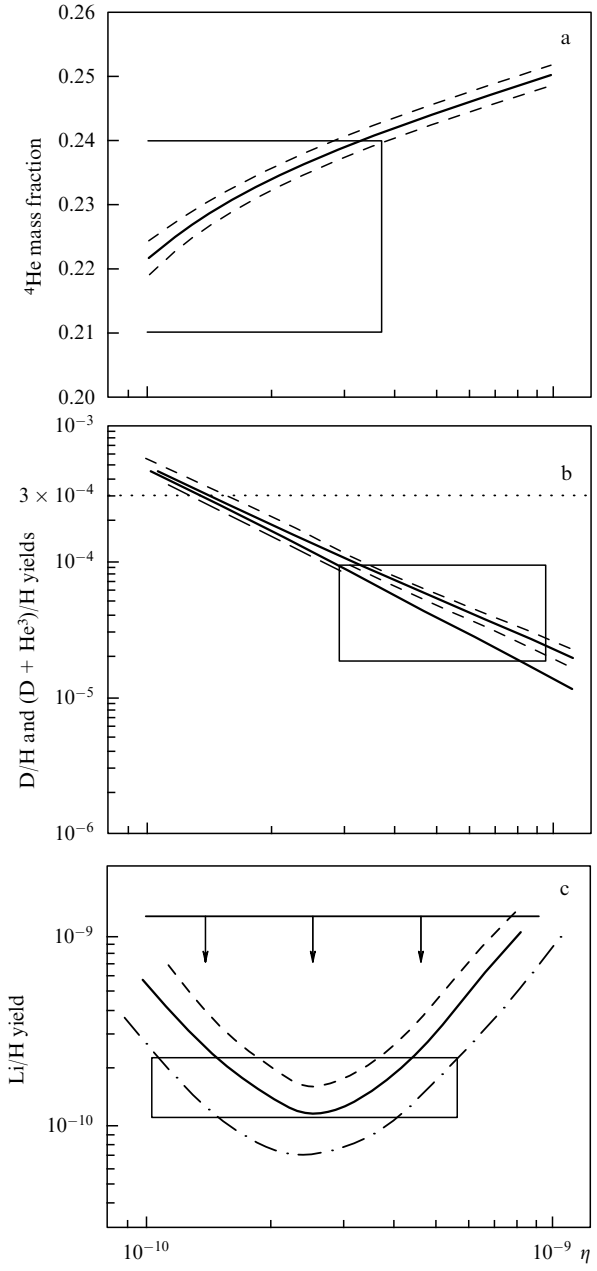

Figure 9. Light element yields as a function of the baryon-to-photon ratio η: (a) ^{4}He, (b) D/H + ^{3}He/H, (c) ^{7}Li/H [1]. Rectangles indicate the observed yield ranges.

by the Keck telescope which discovered deuterium spectral absorption lines in galactic hydrogen clouds along the line of sight before a distant high-redshift quasar with poor metal abundance: $D/H = (1.9-2.5) \times 10^{-4}$ [14, 15]. Presumably, in such 'old' objects like quasars the observed value of D/H reflects the primordial yield D_{BB}. So unless the observed spectra have been distorted along the ray path in another hydrogen cloud with 'unfavorable' velocity, one may state that the genuine primordial deuterium yield is observed there (see Table 1).

The pre-solar deuterium yield is larger than its modern abundance due to its destruction in reaction D(p, γ) ^{3}He and smaller than the primordial yield D_{BB} if no deuterium creation occurs in stellar evolution. These results are confirmed by the data shown in Table 1. As follows from

Table 1.

Yields	Galaxy formation $[(D/H)_{BB}]$	Sun formation	Present time
D/H	$(1.9-2.5) \times 10^{-4}$	$(2.6 \pm 1.0) \times 10^{-5}$	$(1.6 \pm 0.1) \times 10^{-5}$
metals	0	$\approx 2 \times 10^{-2}$ [16]	

Table 1, deuterium has been destroyed by about an order of magnitude over galactic history.

b) Primordial D + ^{3}He. In the absence of information on quasars and due to the large dispersion of D/H observed in the ISM and uncertainties in chemical evolution effects, the limits to the primordial deuterium yield were usually derived from analysis of the sum of the primordial yields (D + ^{3}He).

The pre-solar yield of ^{3}He, as well as that of deuterium, can be determined from the analysis of carbonaceous chondrites, which are thought to represent the primordial chemical composition of the Solar system. On the other hand, studies of gas-rich meteorites and solar wind observations yield modern ^{3}He abundance, which is a combination of the decayed deuterium and the primordial pre-solar helium-3.

Smith, Kawano and Malany [1] find $D_{BB} > 1.8 \times 10^{-5}$ at a consistency level of 95% and also estimate the (D + ^{3}He) yield using a simple model of chemical evolution of ^{3}He: $(D + {}^3He)_{BB} < 9 \times 10^{-5}$. New observational data on the primordial deuterium yield (see Table 1) clearly contradict to this upper limit, and it must be revised.

c) Primordial ^{3}He. The direct presence of ^{3}He in the solar wind was detected using metallic foils placed on the lunar surface, as well as from spectroscopic observations of solar flares. It is observed in the interstellar medium in HII regions at distances of 20 kpc from the Galactic center due to the superfine transition in $^3He^+$ at a wavelength of 3.46 cm. According to these observations, the typical yield ratio ^{3}He/H lies in the range $2 \times 10^{-5} - 8 \times 10^{-5}$ [1].

The primordial ^{3}He yield cannot be directly determined from these data due to uncertainties in stellar reprocessing of matter containing ^{3}He. Low-mass stars tend to synthesize ^{3}H whereas massive stars destroy it. It is reasonable to suggest that in an early phase of stellar evolution (prior to the main sequence) all primordial D is converted into ^{3}He. This additionally produced ^{3}He together with the primordial survives in stellar layers with temperatures below 7×10^6 K. At higher temperatures ^{3}He burns into ^{4}He. ^{3}He is thought to be additionally created at the hydrogen burning stage (on the main sequence) (see, e.g., Ref. [18]) and is mixed up with the surface material on the low mass red giant branch (RGB) surviving thermal instability phase on the asymptotic giant branch (AGB).

Low mass stars are therefore 'net' producers of ^{3}He in this model. Olive et al. [18] calculated the galactic evolution of ^{3}He for different assumptions of the primordial deuterium yield and found a noticeable overproduction of ^{3}He, which exceeds the solar abundance and yields observed in HII regions, when its formation in low mass stars ($M = 1-3M_\odot$) is taken into account. The reason for this discrepancy, according to the authors [18], lies in the shift of the available observational results toward the region of suppressed ^{3}He abundance near massive stars (see Fig. 10). Therefore, data on ^{3}He provides no possibility to estimate the primordial yield D_{BB} (^{3}He) which can be used to analyze standard BBN parameters.

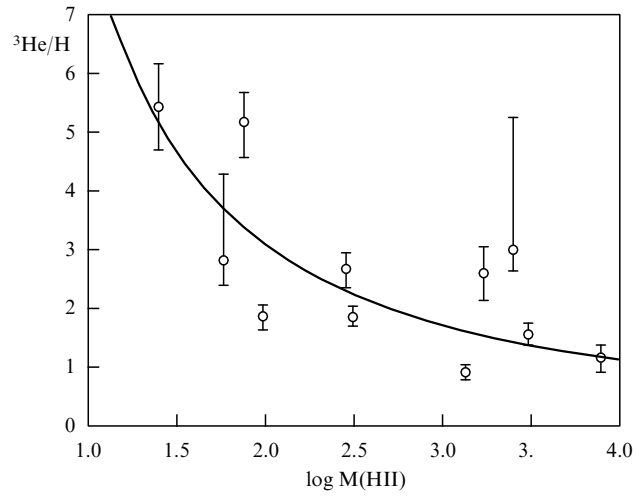

Figure 10. Relative abundance of ^{3}He/H in some galactic HII regions as a function of the region mass [18].

Moreover, recent observations of ^{3}He in planetary nebulae (NGC 3242 and others) [19, 20] give a superhigh value of ^{3}He/H $\sim 10^{-3}$ confirming the complexity in predicting the primordial yield of this nucleus. Below in Section 2 we shall consider ^{3}He abundance and its galactic evolution in more detail.

d) Primordial ^{4}He. ^{4}He abundance can be estimated by various methods: using optical and radio emission lines from galactic nebulae, optical absorption lines in stars, planetary atmosphere data, data from solar oscillation studies, etc. [1]. This is connected with the fact that ^{4}He is a very abundant element in the Universe accounting for about one fourth of its baryon mass. The primordial ^{4}He (Y_{BB}) yield is most reliably determined from analysis of emission lines from poor-metal extragalactic HII regions and dwarf galaxies where helium can be observed through recombination of He^+ ions.

The observed helium abundance in these regions is plotted as a function of 'metallicity', i.e. 'metal' content, which in astrophysics implies the abundance of elements heavier than helium. The obtained curve is extrapolated to zero metallicity, i.e. to the beginning of chemical evolution. The mass fraction of ^{4}He obtained in this way is assumed to be equal to Y_{BB}, the primordial helium yield. An analysis of data on HII regions with metallicity smaller than one fourth of the solar metallicity leads to $Y_{BB} = 0.225 \pm 0.005$ if oxygen is taken as a mark, and to $Y_{BB} = 0.229 \pm 0.004$ if nitrogen is taken [21] (statistical errors are at the 1-σ level). Walker et al. [3] arrived at similar results. Fuller et al. [22] used 14 the most metal-poor objects to derive $Y_{BB} = 0.220 \pm 0.007$ using nitrogen as a mark. Olive and Steigman [23] used recent measurements of ^{4}He in 50 low metal HII regions with nitrogen and oxygen marks to determine a conservative limit to Y_{BB} at the 2-σ level. They notice that the observational data are consistent with $Y_{BB} = 0.232 \pm 0.003$. At the 2-σ level this corresponds to an upper limit $Y_{BB} < 0.238$ or, introducing a systematic error $\sigma_{syst} = \pm 0.005$, $Y_{BBmax} < 0.243$. This estimate agrees with limits derived in Ref. [1]: $0.21 < Y_{BB} < 0.24$.

Systematic errors in observations of ^{4}He may be due to the contribution of collisional excitation of spectral lines, neutral helium, interstellar 'reddening' (spectral line shift towards longer wavelengths), uncertainties in the ionizing ultraviolet radiation flux, etc. All these effects complicate a precise analysis of ^{4}He spectral lines and its abundance estimates.

1.2.2 Comparison with predicted primordial yields. The allowable parameter region obtained from comparison of observed (D + ^{3}He)/H, ^{4}He/H, ^{7}Li/H abundances with predicted primordial yields by Smith, Kawano and Malany [1] is shown in Fig. 11. This region has a lower limit of the primordial (D + ^{3}He) yield and an upper limit of the ^{4}He primordial yield:

$$2.9 < \eta_{10} < 3.8\,. \tag{7}$$

New data on the existence of larger deuterium yields [12] abruptly shift the allowable region to smaller values:

$$\eta < 2 \times 10^{-10}\,. \tag{8}$$

If the primordial deuterium yield is $(1.9-2.5) \times 10^{-4}$ [14, 15], the predicted yields of ^{4}He and ^{7}Li lie within the ranges

$$Y_{BB}(^4\mathrm{He}) = 0.228-0.236\,,\ (^7\mathrm{Li/H})_{BB} = (0.8-3.5) \times 10^{-10},$$

respectively, which are in good agreement with direct estimates [1]

$$Y_{BB}(^4\mathrm{He}) = 0.228 \pm 0.003\,,$$
$$(^7\mathrm{Li/H})_{BB} = (1.1-2.3) \times 10^{-10}\,.$$

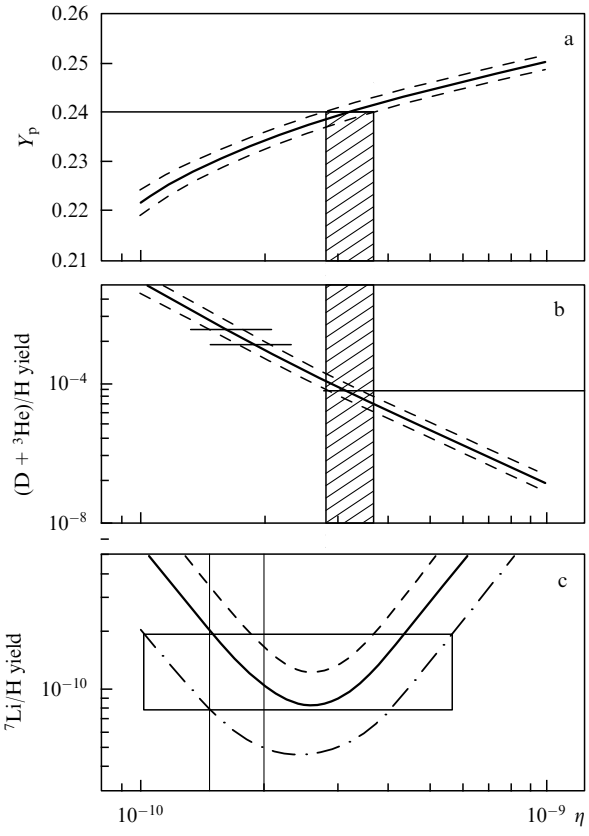

Figure 11. Light element yields as a function of η (the same as in Fig. 9). The hatched region shows the allowable range of η which is consistent with all observational data obtained by 1993 [1].

It should be however noted that at present there is another group of observations indicating a much smaller $(D/H)_{BB} \sim 3 \times 10^{-5}$ [24, 25].

In particular, one of the best recent measurements of D/H for the quasar Q 1937 + 1009 with a red-shift $Z = 3.572$ gives a value $D/H = (3.3 \pm 0.3) \times 10^{-5}$ [26]. Analysis and measurements of Ref. [27] also give a high value of D/H. At the same time, the data of [14,15] are confirmed in Ref. [28]. Thus the situation regarding the evaluation of $(D/H)_{BB}$ remains ambiguous.

We consider now in more detail the data on ^{3}He in connection with its chemical evolution in the Galaxy.

2. Chemical evolution of deuterium and ^{3}He in the Galaxy

As indicated in Section 1.2, ^{3}He is the most difficult isotope to compare the observed abundance with predicted primordial yield because ^{3}He is simultaneously created and destroyed in stars. As we have seen above, its stellar re-processing is very sensitive to the initial mass of the star. The dependence of the ^{3}He yield on the initial stellar mass shown in Fig. 12 is obtained from a simple estimate of ^{3}He survival at temperatures $T < 7 \times 10^6$ K. Denoting the fraction of ^{3}He which has survived in stellar interiors by g_3, the yield of ^{3}He by the time t is described by the relation:

$$(^3\mathrm{He/H})_t > g_3\left[(\mathrm{D} + {}^3\mathrm{He})/\mathrm{H}\right]_\mathrm{p} - g_3(\mathrm{D/H})_t\,. \qquad (9)$$

Here D + ^{3}He increases with time if $g_3 > 1$ and decreases if $g_3 < 1$.

Before paper [18] appeared, the production of ^{3}He in low mass stars had usually been neglected in analysis of ^{3}He chemical evolution by choosing $g_3 < 1$. The different fate of ^{3}He in high and low mass stars is due to the fact that in stars with $M < 2M_\odot$ p-p hydrogen burning dominates and ^{3}He is produced by the reactions

$$\mathrm{p(p,\nu e^+)D(p,\gamma)}{}^3\mathrm{He}\,, \qquad (10)$$

while for stars with $M > 2M_\odot$ the CNO-cycle dominates and ^{3}He is destroyed [26–28]. Taking into account the effect of ^{3}He production in low mass stars on g_3, Olive et al. [18] considered three models of ^{3}He chemical evolution with different values of the primordial yields:

1. $(D/H)_{BB} = 7.5 \times 10^{-5}$, $g_3 = (2.7; 1.2; 0.9)$;
2. $(D/H)_{BB} = 2.5 \times 10^{-4}$, $g_3 = (1.4; 0.9; 0.8)$;
3. $(D/H)_{BB} = 3.5 \times 10^{-5}$, $g_3 = (4.4; 1.6; 1.1)$. (11)

Here the three values of g_3 correspond to three masses of stars which are 'net' ^{3}He producers: $M = 1; 2; 3M_\odot$.

The results obtained for the chosen parameters are presented in Fig. 13. As seen from this figure, overproduction of ^{3}He with respect to the solar abundance is obtained in all three models. The largest discrepancy arises in the model with primordial deuterium yield $(D/H)_{BB} = 2.5 \times 10^{-4}$, which is actually observed in quasars [14,15]. This is the present-day enigma of ^{3}He.

Paper [18] also notes that the observed dispersion of the ^{3}He abundance relative to the mass of galactic HII regions can be explained by the destruction of ^{3}He by short-lived high

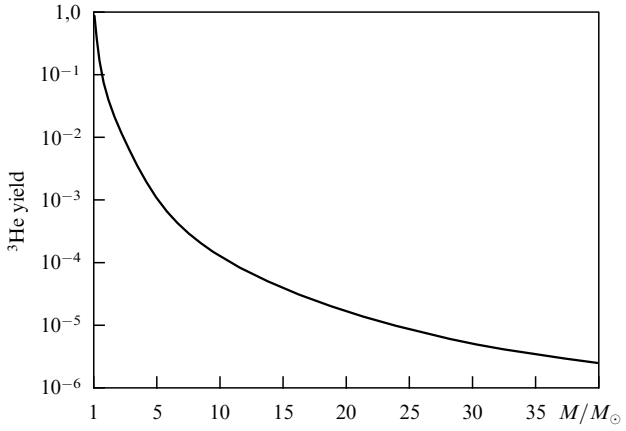

Figure 12. Differential yield of ^{3}He as a function of stellar mass [18].

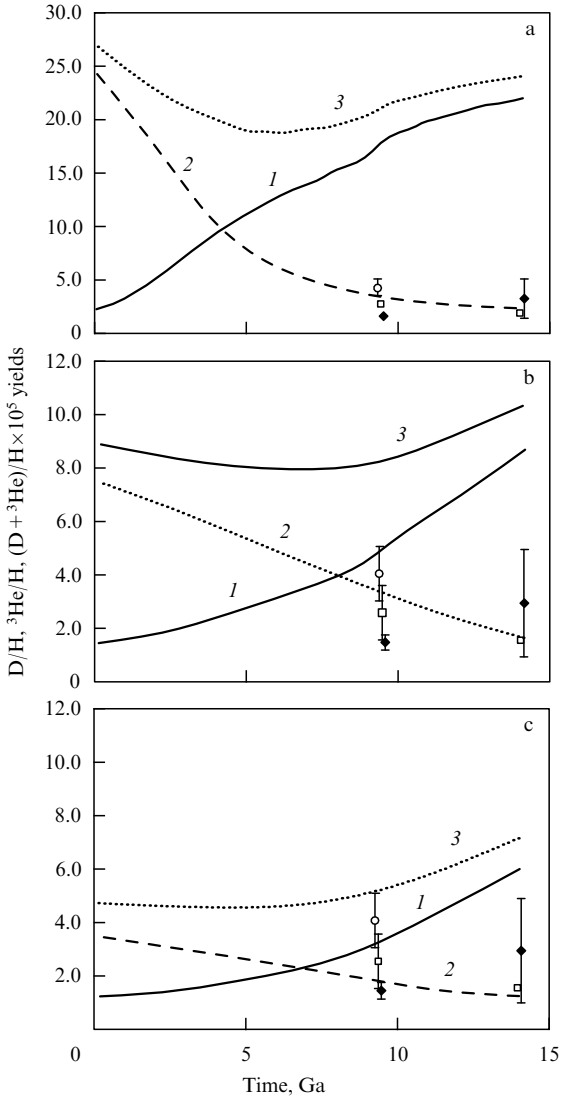

Figure 13. Evolution of light element yields as a function of time in models with 'net' production of ^{3}He in low mass red giants [18]. *1* — ^{3}He/H, *2* — D/H and *3* — (D + ^{3}He)/H. The observational data are shown for the Solar system formation epoch ($t = 9.6$ billion years) and at the present time ($t = 14.2$ billion years). D/H — □, ^{3}He/H — ◆, (D + ^{3}He)/H — ○. The primordial deuterium yields are (a) $(D/H)_{BB} = 7.5 \times 10^{-5}$, (b) $(D/H)_{BB} = 2.5 \times 10^{-4}$, (c) $(D/H)_{BB} = 3.5 \times 10^{-5}$.

mass stars and the production of ^{3}He in low mass stars. Thus when estimating the BBN yield of ^{3}He we should rather trust in the sparse data on low mass galactic HII regions than on massive regions. Low mass regions explain the modern ^{3}He abundance. This is confirmed by the high values of ^{3}He/H obtained from observations of ^{3}He in planetary nebulae [19, 20].

Recently Olive et al. [32] considered new models of chemical evolution of D and ^{3}H in which D can be significantly destroyed but no 'heavy' element overproduction is obtained. These models are based upon calculations of matter ejection in supernova explosions [33]. It was found that the result of analysis of the chemical evolution of ^{3}He significantly depend on the state of the star during the red giant phase. If there is rotational mixing at this stage [34], some low mass stars, which produce ^{3}He before the main sequence, turn out to be 'net' destroyers of ^{3}He. Such destruction of ^{3}He occurs already after the main sequence so the evolutionary curves obtained in previous calculations of Olive et al. [18] (see Fig. 13) are correct only for net helium-3 creation on the main sequence. With account of ^{3}He destruction effects [34] not only by high mass stars but also due to rotational mixing in low mass stars, the picture of chemical evolution of ^{3}He changes, so we can obtain a consistency between its yield in the Solar system formation epoch and at the present time (Fig. 14). It should be noted, however, that such calculations (Fig. 14) do not explain the high ^{3}H/H ratio obtained in planetary nebulae. So the possibility remains that some fraction of stars with masses $1-3\ M_\odot$ do not destroy their ^{3}He after the main sequence.

3. Is the problem of ^{3}He production galactic or cosmological?

3.1 ^{3}He in red giants

The most solid proof of the additional production of ^{3}He in stars (or its higher primordial yield) follows from observations of this isotope in galactic planetary nebulae. As noted above, the first detection of ^{3}He in NGC 3242 [19] showed that low mass stars can be intensive producers of ^{3}He. The observed yield $^3\mathrm{He/H} \sim 10^{-3}$ in NGC 3242 and other nebulae is in a good qualitative agreement with calculations for stars with $M \sim M_\odot$ [20]. At the same time, since the observed abundance in the ISM is $^3\mathrm{He/H} \sim 10^{-5}$, a question naturally arises as to whether the above-mentioned galactic nebulae are exceptional or they reflect the nature of ^{3}He evolution in low mass stars. The anomalously low $^{12}\mathrm{C}/^{13}\mathrm{C}$ ratios observed in many red giants confirm the possibility of strong mixing and thus ^{3}He destruction. However, as noted in Ref. [20], this mechanism is effective only in stars with a mass less than two solar masses.

We recall that a red giant is a star with helium core around which thermonuclear hydrogen burning proceeds in a thin layer, or a star with carbon–oxygen core surrounded by two burning layers, hydrogen and helium. In the extended cool envelopes of red giants energy is transported by convection which lifts up nuclear burning products from unstable thin layers into the atmosphere of the star. Red giants are characterized by a strong mass outflow into interstellar space (called a 'stellar wind'). The stellar wind composition is determined by the mixing that occurs in the outer layers of red giants when the hydrogen (i.e. proton) burning shell moves outwards, which lead to the enrichment of carbon

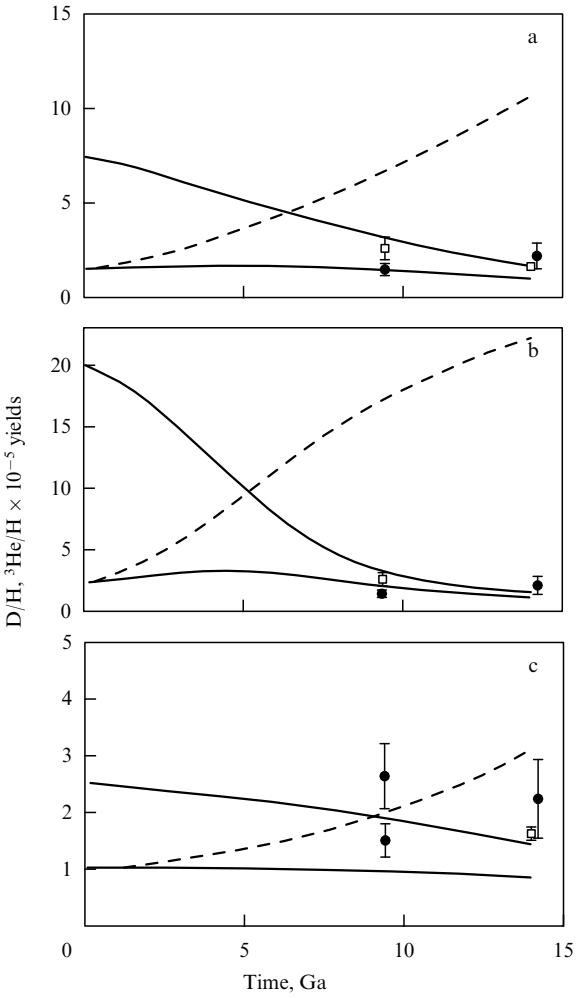

Figure 14. Evolution of D/H and ^{3}He/H yields as a function of time in models with destruction and production of ^{3}He in low mass red giants [29]. The primordial deuterium yields are (a) $(D/H)_{\mathrm{BB}} = 7.5 \times 10^{-5}$, (b) $(D/H)_{\mathrm{BB}} = 2 \times 10^{-4}$, (c) $(D/H)_{\mathrm{BB}} = 2.5 \times 10^{-5}$.

with ^{13}C nuclei through the reaction

$$^{12}\mathrm{C} + \mathrm{p} \rightarrow {}^{13}\mathrm{N}(\mathrm{e}^+\nu) \rightarrow {}^{13}\mathrm{C}\,. \qquad (12)$$

Galli et al. [20] suggested an explanation of the ^{3}H enigma at the 'stellar level' as follows:

1. Stars with masses less than $2M_\odot$ destroy ^{3}He after the main sequence stage providing ^{3}He-poor matter into the ISM, which is consistent with the low ^{3}He/H ratio measured in presolar matter in galactic HII regions and circumsolar space.

2. High yields of ^{3}He in planetary nebulae are due to their progenitor mass being higher than $2M_\odot$ or due to a mechanism preventing strong matter mixing.

They analyzed planetary nebulae with measured ^{3}He yields and found that the progenitor masses of these planetary nebulae do not exceed $2.5M_\odot$. Figure 15 shows the calculated ^{3}He yield as a function of the progenitor mass for six planetary nebulae, and presents the observed ranges of ^{3}He/H. The calculations were made for a non-standard mixing using the above assumptions.

Therefore these results together with planetary nebula observations do not confirm the assumption about strong ^{3}He depletion for the entire range of low mass stars. Only for $M < 2.5M_\odot$ can high values of ^{3}He/H be obtained.

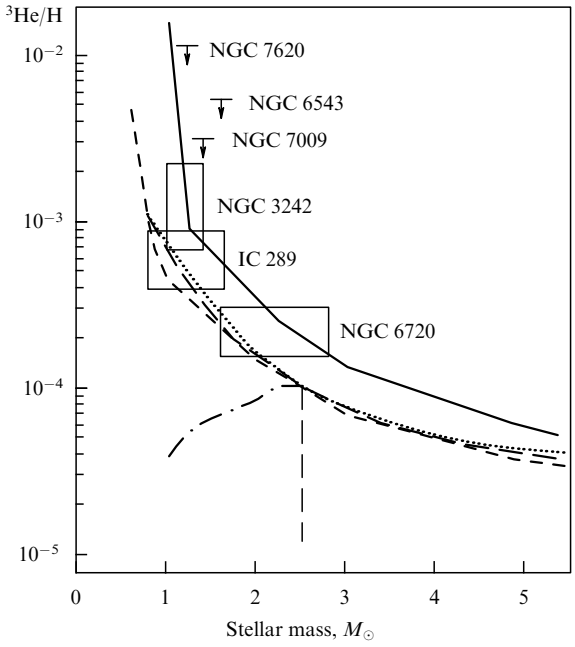

Figure 15. ^{3}He abundance in planetary nebulae as a function of their progenitor masses. The curves show model calculation yields assuming deep matter mixing in red giants with mass $M < 2.5M_\odot$ [2].

3.2 ^{3}He in the primordial nucleosynthesis

As follows from the previous section, the chemical evolution of ^{3}He in the Galaxy cannot provide consistency between observed and predicted ^{3}He abundances. So the 'usefulness of this isotope as a cosmological barometer is highly questionable' [20]. A large ^{3}He abundance in galactic planetary nebulae can imply not only its significant creation in stars, but also probably its additional formation in the primordial nucleosynthesis.

The authors of this review have recently pointed to the possible role of neutrinos to increase ^{3}He production due to the exothermic reaction with tritium [35]:

$$\nu + {}^3\mathrm{H} \rightarrow {}^3\mathrm{He} + \mathrm{e}^- . \qquad (13)$$

If the primordial nucleosynthesis occurred a sufficiently long after the moment of 'decoupling' of weak interaction reactions

$$\mathrm{n} + \mathrm{e}^+ \rightarrow \mathrm{p} + \bar{\nu}, \quad \mathrm{p} + \mathrm{e}^- \rightarrow \mathrm{n} + \nu , \qquad (14)$$

the neutrino flux is relatively small for reaction (13) to be important. However, if the decoupling is close to the nucleosynthesis, the neutrino flux is nearly 'equilibrium', i.e. the number of neutrinos is approximately equal to the number of protons. This can be achieved, for example, if the rate of weak interactions in the early Universe is different from the contemporary one [36]. In this case, assuming for the primordial nucleosynthesis (Fig. 8) that ^{3}H and ^{3}He formation channels in reactions with neutrons (D + n) and protons (D + p) are equally important, we arrive at

$$\frac{(^3\mathrm{He})_{\nu+\mathrm{T}}}{(^3\mathrm{He})_{\mathrm{D+p}}} = 1 - \exp(-\sigma_\nu f_\nu) . \qquad (15)$$

Here $\sigma_\nu \sim 10^{-44}$ cm^2 $(E_\nu/m_\mathrm{e}c^2)^2$ is the neutrino capturing cross-section by tritium, f_ν is the integral neutrino flux, E_ν is the energy of the neutrino, and m_e is the mass of electron. For $f_\nu > 10^{43}$ cm^{-2} the fractions of ^{3}He produced by neutrino captures and nuclear reactions with charged particles become comparable. As the size of the Universe by the time of BBN is about $10^{11} - 10^{12}$ cm, such neutrino fluxes seem to be realistic. As a result, an ^{3}He increase is obtained due to this additional formation channel. Yet the yield of ^{4}He remains practically the same due to a close cycle of reactions leading to its formation. Contributions of other possible reactions with neutrinos or antineutrinos, such as

$$\nu + \mathrm{D} \rightarrow \mathrm{p}^+\mathrm{p}^+\mathrm{e}^-, \quad \bar{\nu} + \mathrm{D} \rightarrow \mathrm{n} + \mathrm{n} + \mathrm{e}^+ ,$$
$$\bar{\nu} + {}^3\mathrm{He} \rightarrow {}^3\mathrm{H} + \mathrm{e}^+ , \qquad (16)$$

at $T \sim 1$ MeV are negligibly small compared with reaction (13), so they cannot alter the deuterium and helium-4 yields.

These considerations require primordial nucleosynthesis calculations with changing input parameters, such as the moment of weak interaction equilibrium 'decoupling' or the value of the neutron-to-proton ratio, which may be different from values used in inhomogeneous primordial nucleosynthesis models.

Another possible mechanism for additional formation of D and ^{3}He by the end of the primordial nucleosynthesis was considered by M Yu Khlopov and V M Chechetkin. The mechanism is based on the annihilation of ^{4}He nuclei interacting with antiprotons [4]. Antiprotons can appear in the Universe at $10^2 < t < 10^{13}$ s due to the decay of metastable particles, the evaporation of primordial black holes, and the presence of antimatter domains. Deuterium, helium-3 and tritium are formed in the reactions

$$\bar{\mathrm{p}} + {}^4\mathrm{He} \rightarrow \begin{array}{l} \mathrm{D} + \mathrm{p(n)} + N(\pi) , \\ {}^3\mathrm{He} + N(\pi) , \\ {}^3\mathrm{He} + N(\pi) , \end{array} \qquad (17)$$

where $N(\pi)$ is a number of pions.

The destruction of even a tiny fraction of ^{4}He($\sim 10^{-4}$) by annihilation with antiprotons can lead to almost the total observed abundance of D and ^{3}He. For the concentration $^3\mathrm{He/H} = 4 \times 10^{-5}$ the restriction on the antiproton-to-proton number ratio obtained in Ref. [5] becomes $N(\bar{\mathrm{p}})/N(\mathrm{p}) < 2.5 \times 10^{-3}$.

An additional indirect formation mechanism for D, ^{3}H, and ^{3}He by the annihilation $\bar{\mathrm{p}} + {}^4\mathrm{He}$ arises at sufficiently high densities of matter. Free neutrons formed in the reaction $\bar{\mathrm{p}} + {}^4\mathrm{He} \rightarrow \mathrm{D} + \mathrm{n} + N(\pi)$ can interact with protons and deutons before decay thus producing deuterium and tritium, respectively. In turn, protons can produce ^{3}He through the reaction $\mathrm{p} + \mathrm{D} \rightarrow {}^3\mathrm{He} + \gamma$. This necessitates experimental studies of ^{3}He and D yields in reactions $\bar{\mathrm{p}} + {}^4\mathrm{He}$.

4. Conclusions

Galli et al. [20] showed that the account of ^{3}He destruction in low mass red giants does not significantly change its yield in the Galactic history. So they try to overcome the difficulties in explaining large values of D/H observed in quasar absorption lines and large ^{3}He abundances in planetary nebulae using 'galactic arguments'. This is one possible means of solving the helium-3 problem.

Another way to solve it may be using non-standard BBN models.

This work was supported by a grant from the Kosmion Scientific Studies Centre and from the V G Khlopin Radium Institute.

References

1. Smith M S, Kawano L N, Malany R A *Astroph. J. Suppl.* **85** 219 (1993)
2. Zel'dovich Ya B, Novikov I D *Stroenie i Evolyuthija Vselennoĭ* (Structure and Evolution of the Universe) (Moscow: Nauka, 1975)
3. Walker T P et al. *Astrophys. J.* **376** 51 (1991)
4. Kramarovskiĭ Ya M, ChechevV P *Sintez Elementov vo Bselennoĭ* (Syntehsis of Elements in the Universe) (Moscow: Nauka, 1987)
5. Khlopov M Yu, ChechetkinV M *EChAYa* **18** (3) 627 (1987)
6. Bisnovatyi-Kogan G S, ChechetkinV M *Pis'ma Zh. Eksp. Teor. Fiz.* **17** 662 (1973) [*JETP Lett.* **17** 447 (1976)]
7. Epstein R I, Lattimer J M, Schramm D N *Nature* (London) **263** 198 (1976)
8. Geiss J, in *Origin and Evolution of the Elements* (Eds N Prantzos, E Vangioni-Flam, M Casse) (Cambridge: Cambridge Univ. Press, 1993) p. 79
9. Beer R et al. *Science* **175** 1360 (1972)
10. Jefferts K B, Penzias A A, Wilson R W *Astrophys. J.* **179** L57 (1973)
11. Spitzer L et al. *Astrophys. J.* **181** L116 (1973)
12. Rogerson J B, York D C *Astrophys. J.* **186** 95 (1973)
13. Linsky J L et al. *Astrophys. J.* **402** 694 (1992)
14. Songaila A et al. *Nature* (London) **368** 599 (1994)
15. Carswell R F et al. *Monthly Not. R. Astron. Soc.* **278** 518 (1996)
16. Anders E, Grevesse N *Geochim. Cosmochim. Acta* **53** 197 (1989)
17. Vangioni-Flam E, Casse M *Astrophys. J.* **441** 471 (1995)
18. Olive K A et al. *Astrophys. J.* **444** 680 (1995)
19. Rood R T, Bania T H, Wilson T L *Nature* (London) **355** 618 (1992)
20. Galli D et al. *Astroph. J.* **477** 218 (1997)
21. Pagel B E J et al. *Phys. Scripta* **36** 7 (1991)
22. Fuller G M, Boyd R N, Kalen J D *Astrophys. J. Lett.* **371** L11 (1991)
23. Olive K A, Steigman G *Astroph. J. Suppl.* **97** 49 (1995)
24. Tytler D, Fan X-M, Burles S *Nature* (London) **381** 207 (1996)
25. Burles S, Tytler D *Astrophys. J.* **460** 584 (1996)
26. Burles S, Tytler D, astro-ph/9712108
27. Levshakov S A, Kegel W H, Takahara F, astro-ph/9712305, in Particle Cosmology (Eds K Sato, T Yangida, T Shiromizu) (Tokyo: Universal Academy Press, Inc., 1997); Levshakov S A, Takahara F, Kegel W H, astro-ph/9712136
28. Rugers M, Hogan C J *Astrophys. J. Lett.* **459** L1 (1996)
29. Iben I Jr., Truran J W *Astrophys. J.* **220** 980 (1978)
30. Fields B D, Olive K A *Phys. Lett. B* **368** 103 (1996)
31. Dearborn D S P, Schramm D N, Steigman G *Astrophys. J.* **302** 35 (1986)
32. Olive K A et al. *Astrophys. J.* **479** 752 (1997)
33. Scully S et al. *Astrophys. J.* **476** 521 (1997)
34. Boothroyd A I, Malaney R A, astro-ph/9512133 (see Ref. [32])
35. Kramarovskiĭ Ya M, ChechevV P, in *Proc. 48th Conference on Nuclear Spectroscopy and Atomic Nucleus Structure, June 16 – 19 1998, M*. p. 148.
36. Kramarovskiĭ Ya M, Levin B M, Chechev V P *Nuclear Physics* **55** (2) 441 (1992)